ADVANCED FUNCTIONAL MATERIALS

FULL PAPER

DOI: 10.1002/adfm.200601136

Mechanical Properties of Robust Ultrathin Silk Fibroin Films**

By *Chaoyang Jiang*, *Xianyan Wang*, *Ray Gunawidjaja*, *Yen-Hsi Lin*, *Maneesh K. Gupta*, *David L. Kaplan*, *Rajesh R. Naik*, *Vladimir V. Tsukruk**

Robust ultrathin multilayer films of silk fibroin were fabricated by spin coating and spin-assisted layer-by-layer assembly and their mechanical properties were studied both in tensile and compression modes for the first time. The ultrathin films were characterized by a high elastic modulus of 6–8 GPa (after treatment with methanol) with the ultimate tensile strength reaching 100 MPa. The superior toughness is also many times higher than that usually observed for conventional polymer composites (328 kJ m^{-3} for the silk material studied here versus typical values of < 100 kJ m^{-3}). These outstanding properties are suggested to be caused by the gradual development of the self-reinforcing microstructure of highly crystalline β-sheets, serving as reinforcing fillers and physical crosslinks, a process that is well known for bulk silk materials but it is demonstrated here to occur in ultrathin films as well, despite their limited dimensions. However, the confined state within films thinner than the lengths of the extended domains causes a significantly reduced elasticity which should be considered in the design of nanosized films from silk materials. Such regenerated silk fibroin films with outstanding mechanical strength have potential applications in microscale biodevices, biocompatible implants, and synthetic coatings for artificial skin.

1. Introduction

Biocompatible materials have received increased interest due to their combination of unique physical, chemical, and biological properties and their potential in the fields of drug delivery, medical treatments, and other biological applications.[1–5] Among the natural polymers,[6] silkworm silk fibroin has been of interest for its use in textiles but also in consumer products such as cosmetic creams, lotions, makeup, and pharmaceuticals.[7] Silkworm silk fibroin has been used commercially as biomedical sutures for decades. The incorporation of silk into medical textiles such as artificial tendons, blood vessels, and skin grafts is attractive because the protein exhibits excellent biocompatibility in vivo.[8–10] Promising results regarding this feature have been demonstrated both in vitro and in vivo.[11–14] Silk fibroin from the silkworm *B. mori* has been dissolved and then reformulated into new materials, with the ability to control the crystalline state (beta-sheet content) and morphology, in order to modulate the mechanical properties and the rate of extent of degradation.[13,15–18] The outstanding mechanical properties of silk fibers are characterized by high strength (ca. 3 GPa) combined with high extensibility (ca. 30 %), and good compressibility.[19–25] Moreover, they are mechanically stable up to 200 °C under dynamic mechanical evaluations.[21] With these excellent mechanical properties, silk proteins have become candidates as strong biomaterials that can be applied in various fields of controlled release and scaffolds for tissue engineering, where a combination of high strength and elasticity are often required.

To fabricate uniform thin and ultrathin polymeric films spin casting and layer-by-layer (LbL) assembly are widely utilized. Spin casting represents the easier fabrication method (100–1000 nm thick films) for ultrathin silk films while LbL assembly allows for the fabrication of ultrathin (1–100 nm) multilayered films in a step-wise manner similarly to that developed for electrostatically driven LbL. Depending on the nature of components and fabrication conditions, inter-layer interactions may be electrostatic, hydrogen bonding, van der Waals interactions, and short-range hydrophobic interactions. Stepwise deposition, an expansion of the classical LbL assembly, was demonstrated for the fabrication of silk fibroin multilayer films because of their short-range hydrophobic interactions.[16] Although LbL assembly has become a versatile approach widely applied to the fabrication of biosensors, controlled drug delivery, superhydrophobic surfaces, fuel-cell membranes, and elec-

[*] Prof. V. V. Tsukruk, Dr. C. Jiang, R. Gunawidjaja, Y.-H. Lin
School of Materials Science and Engineering
Georgia Institute of Technology
Atlanta, GA 30332 (USA)
E-mail: vladimir@mse.gatech.edu
Dr. X. Wang, Prof. D. L. Kaplan
Department of Biomedical Engineering
Tufts University
Medford, MA 02155 (USA)
Y.-H. Lin
Department of Materials Science and Engineering
Iowa State University
Ames, IA 50011 (USA)
M. K. Gupta, Dr. R. R. Naik
Materials and Manufacturing Directorate
Air Force Research Laboratory
Wright-Patterson Air Force Base, OH 45433 (USA)

[**] Some experiments were conducted at Iowa State University, Ames, Iowa. This work is supported by the AFOSR, F49620-03-1-0273 and FA95500410363 and NSF-CBET-0650705 Grants. We thank Dr. K. J. Wahl (NRL) for fruitful discussion.

troluminescent devices,[26–30] technological drawbacks include tedious multi-step routines that limit their more widespread use. However, the recent introduction of spin-assisted LbL (SA-LbL)[31] which combines conventional spin casting and LbL principles have made this approach more efficient by cutting down the time required for fabrication about ten-fold, resulting in expanded applications for these ultrathin films.[32–35]

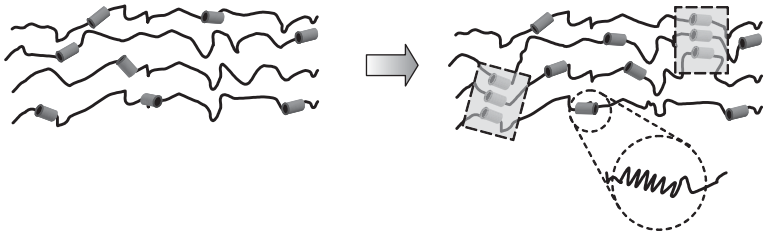

Figure 1. Cartoon image of β-sheet formation in the silk fibroin LbL nanomembrane. The spin-coating process caused an increase of β-sheet content and enhancement of inter-molecular interactions.

The assembly of thin (below 1 μm) and ultrathin (below 100 nm) regenerated silk fibroin films and investigation of their mechanical properties can be of great interest for a wide range of applications and is essential for the fabrication of robust materials in the form of ultrathin films with excellent strength and elasticity combined with tunable biodegradable properties. However, there are few reports on the mechanical properties of silk fibroin films (mainly with nano-indentation), because of the difficulty in fabricating uniform ultrathin films and the limited approaches for measuring their micromechanical properties. Challenges in micromechanical testing of ultrathin organic films are very well known and, in the case of silk materials, no single study offered any firm data on their mechanical behavior especially in both tensile and compressive modes. Even in some studies that have been reported on the fabrication of relatively uniform ultrathin silk films[8,16] the question of mechanical properties of these films and their relationship to the fabrication conditions has not been addressed at all. A general assumption that these mechanical properties and the corresponding processes of the molecular reinforcement (formation of β-sheets) are identical to those in the bulk state (scaled to the film thickness) is not validated. In fact, this behavior is significantly affected by the very limited thickness of a single stratum (< 10 nm), which is well below the domain dimensions, and the overall thickness of the films (100+ nm), which is comparable to the molecular and domain dimensions. The presence of air–film surfaces could severely affect the ability of the macromolecular backbone (total length in the extended state reaching 2 μm[2]) to crystallize and limit the conformation transformations responsible for the ultimate mechanical behavior of these materials.

In this study, both spin casting and SA-LbL assembly were exploited to fabricate thin (500 nm) and ultrathin (20–100 nm) silk fibroin films and these films were tested for tensile and compressive mechanical properties for the first time. The silk films were characterized for elastic modulus, elongation to break, and toughness by applying both bulging tests and buckling measurements. The mechanical parameters in both compressive and tensile modes have been revealed for such ultrathin silk films for the first time and are compared with known properties of the bulk materials. Structural control of the silk protein was gained through physical crosslinks (β-sheets), resulting in robust and stable ultrathin material coatings with excellent mechanical characteristics that do not require specific chemical or photoinitiated crosslinking reactions (Fig. 1). This study demonstrates that this approach, which is well-known for bulk silk material, can be successfully applied to ultrathin silk films with thicknesses comparable to chain dimensions resulting in much stronger materials while crystallization progresses. However, even if this result can be taken as an indication that these highly confined conditions do not disturb significantly the β-sheet formation on the nanoscale and their role in the enhancing overall mechanical strength and toughness, the highly reduced overall elasticity of the ultrathin silk films points to significant hindering of the overall conformational flexibility of the long-chain backbones under confined conditions.

2. Results and Discussion

2.1. Spin-Cast Thin Films

For the spin-casting fabrication we used an ionic-liquid solution, which is considered to be more technological and practical because limited solubility can affect the quality of the cast films.[18] Silk films prepared here are stable in organic solvents, such as toluene and acetone, and, after treatment with methanol, their resistance to water treatment increases dramatically resulting in no obvious signs of dissolution observed after water treatment.

The spin-cast films from the silk ionic-liquid solution obtained here were macroscopically smooth and uniform as seen from a typical AFM image of the edge region of a silk fibroin film on a silicon substrate (Fig. 2a). At higher magnification occasional islands were found on the film surface which indicated some aggregation of material in solution prior to spin casting, however, the overall surface was relatively smooth with a surface micro-roughness of 19 ± 5 nm (Fig. 2b).

The thickness of the spin-cast films was 480 ± 30 nm with an overall thickness that can be tuned by the spinning conditions, such as solution concentration, spin speed, and time. Figure 2c shows the dependence of the thickness of 6-layers silk films (methanol treated) upon the speed of spin coating. By increasing the spin speed, a thinner film can be obtained. Here, we report on films obtained with one set of specific parameters which generated uniform films with consistent mechanical response. Rinsing freshly formed spin-cast films with water significantly reduced the film thickness due to the partial removal of water-soluble material that had not completely cured and locked in the beta-sheet crystals to promote full stability in water.

ADVANCED FUNCTIONAL MATERIALS

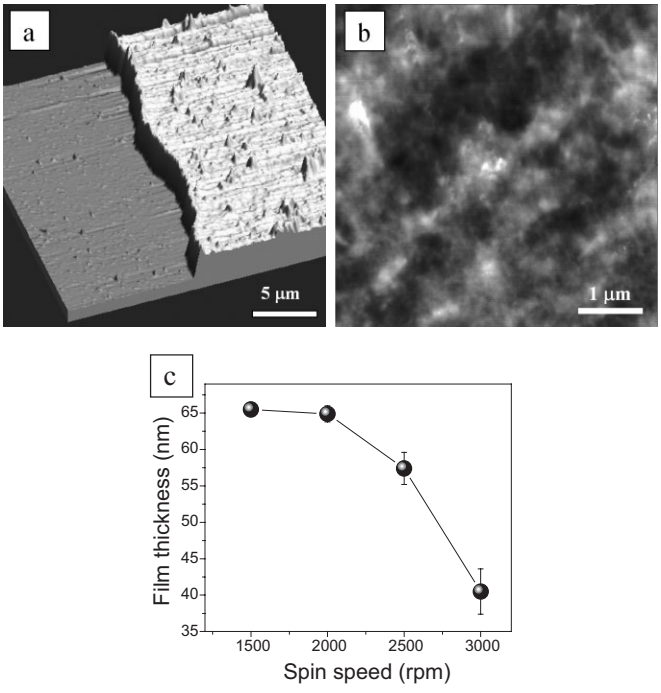

Figure 2. AFM images of methanol-treated silk fibroin (from ionic-liquid solution) formed by spin-casting free-standing films deposited onto a silicon substrate. a) 3D AFM topography image (20 μm × 20 μm) of the edge of the silk film. b) Closer morphology of silk film (5 μm × 5 μm), *Z* scale = 50 nm. c) Thickness dependence of silk LbL films on the speed of spin-coating during the fabrication.

The thickness of the multilayered silk fibroin films deposited on the silicon substrates increased linearly with increasing number of layers deposited, confirming the step-wide growth of the films with a constant increment in total layer thickness (Fig. 4). The error bars are relatively small and reflect the variation of the film thickness obtained for at least three independent fabrication procedures under identical conditions. This linear deposition was also observed in our previous studies using LbL assembly with comparable but slightly different thicknesses.[16] The difference in the thicknesses as compared to our previous studies is due to the different fabricating methods (dipping LbL method used previously versus spin-assisted LbL assembly used in this study) which affected the rate of drying and spreading of the silk materials.[16]

The increase in film thickness after treatment with methanol to initiate crystallization was about 8.6 nm per layer, which is thicker than that routinely observed for synthetic polymers used for usual polyelectrolyte LbL assembly.[30] This is likely because of the unique structure of the silk fibroin protein with its multidomain composition and bulky assemblies of β-sheets. Gentle rinsing with nanopure water prior to methanol treatment resulted in a detectable decrease in film thickness, with the thickness of the uppermost layer shrinking to 7.2 nm because of partial removal of the topmost weakly attached surface aggregates (Fig. 4).

2.2. SA-LbL Ultrathin Films

Ultrathin silk films were fabricated from silk aqueous solution by SA-LbL assembly. Unlike for traditional polyelectrolyte LbL multilayers, where there are strong charge inter-layer interactions, the driving force for the assembly of silk fibroin LbL multilayers is mainly short-range hydrophobic interactions as we have previously reported.[16] These ultrathin films are not soluble in either water or organic solvents. The surface morphology of an SA-LbL silk fibroin film along the edge of the film is shown in Figure 3. The surface of the SA-LbL silk fibroin films was relatively smooth, as observed in large-scale images (Fig. 3a). Higher resolution revealed a granular morphology with lateral granular sizes reaching a fraction of a micrometer (Fig. 3b). The surface roughness, as measured within an area of 1 μm × 1 μm, was 3 nm, which is similar to that of conventional LbL multilayered films from classical polyelectrolytes.[16] Figure 3c shows a representative profile of an AFM image on the edge of 6-layers of LbL silk fibroin films. The thickness determined from this cross section as well as from surface histograms was about 45 ± 5 nm (Fig. 3d). This thickness was independently confirmed by ellipsometric measurements.

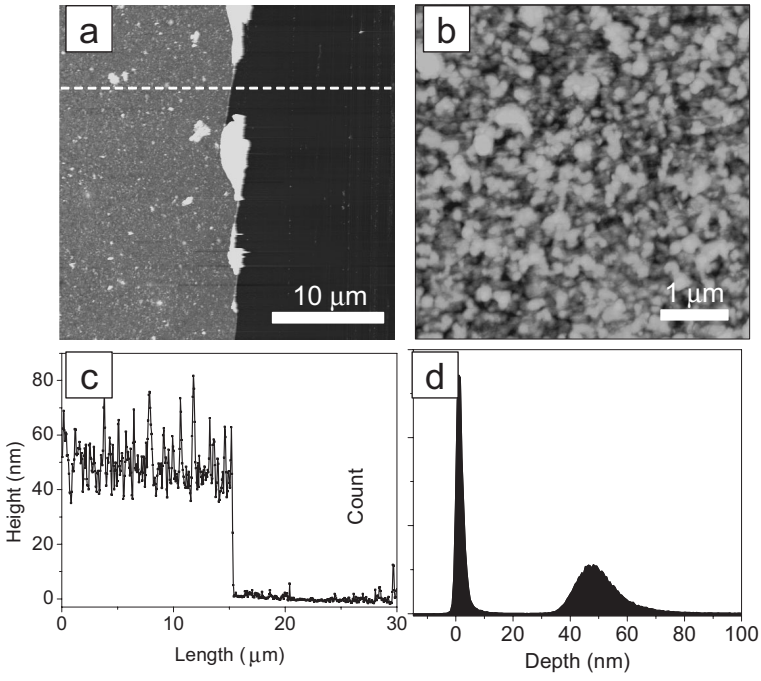

Figure 3. AFM images and data analysis of methanol-treated silk fibroin LbL films (from aqueous solution) on a silicon substrate. a) AFM images of film edge; *Z* scale = 100 nm. b) Closer morphology of silk film, *Z* scale = 200 nm. c) Height profile across the film edge. d) Bearing analysis of the silk film AFM image.

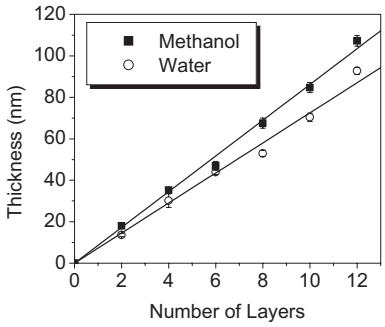

Figure 4. Relationship of the thickness of the silk film and the number of layers to different solvent treatments. Methanol-treated silk films were slightly thicker than the water-treated films.

2.3. Mechanical Properties of Silk Fibroin Films under Compression

To test compressive mechanical properties we exploited the buckling test for thin silk films transferred on a compliant poly(dimethylsiloxane) (PDMS) substrate, which was subjected to controlled compression. Buckling tests, based on the analysis of the buckling instability of ultrathin films on a compliant substrate has been widely exploited because of the simplicity and reliable results with this method.[36–38] This method has also been recently introduced for the measurement of mechanical properties of ultrathin LbL films and showed reproducible results.[39,40] Therefore, to test the mechanical properties of both spin-cast and multilayered films under compressive stresses, free-standing silk films fabricated by the sacrificial-layer method were deposited onto PDMS substrates, compressive stress was applied, and the average spacing of the buckling pattern was determined. The elastic modulus was determined using established equations for stiffer thin films compressed on a compliant elastic substrate.[40]

An optical microscopy image of a compressed spin-cast silk film fabricated as mentioned above and after methanol treatment showed extensive periodic wrinkles with uniform spacing, a typical pattern of buckling instability (Fig. 5a). The corresponding 2D Fast Fourier Transform (FFT) image with a series Fourier components was generated by using Image-J software (see Experimental for details). Both optical images and their 2D FFT images yielded a consistent spacing of 21 ± 2 μm (Fig. 5). The corresponding Young's modulus calculated from this periodicity by applying the known relationship for thin films was 2.8 ± 0.6 GPa, which is a common value for conventional polymers below their glass-transition temperature.[41] Spin-cast films after water treatment did not keep their integrity and could not be transferred to the PDMS substrate for mechanical testing.

Ultrathin multilayered silk films also displayed a buckling instability pattern under compressive stress (Fig. 5). The buckling pattern for ultrathin multilayered films was more uniform and spacing of the wrinkles was smaller, indicating stiffer characteristics for these thinner LbL films when compared to the spin-cast material (Fig. 5b,c). The results of the buckling tests

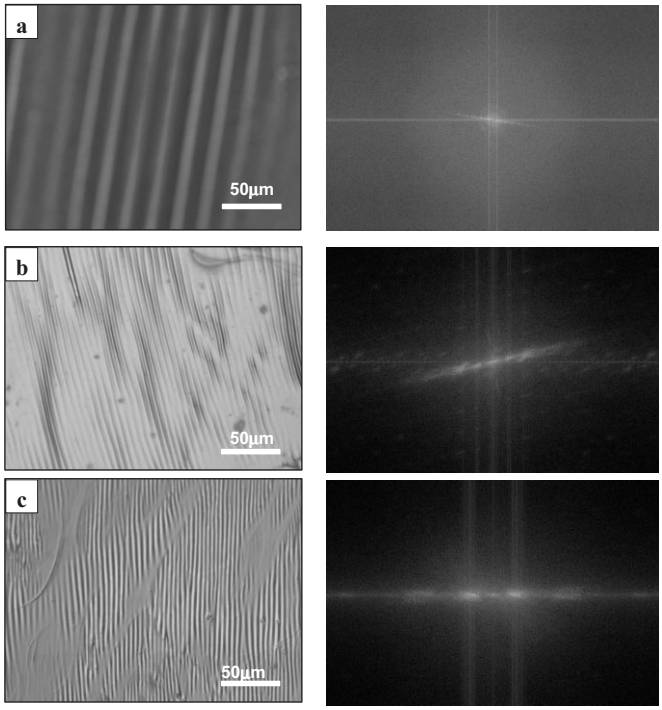

Figure 5. Typical buckling instability patterns for silk fibroin films on a PDMS substrate under compression for a) methanol-treated spin-cast film, b) methanol-treated LbL film, and c) water-treated LbL film. The images at the right-hand side are the corresponding 2D Fourier transformation images of the optical images of these buckling patterns. Each point in the Fourier domain image represents a particular frequency band in a reciprocal space contained in the spatial image. The brighter spots correspond to specific periodicities and can be used to determine the spacing of the buckling patterns.

on silk fibroin films with different fabrication processes are summarized in Table 1. The spacing of the buckling pattern for the multilayer films treated with methanol was 6.1 ± 0.4 μm as determined from the positions of the corresponding bands on the 2D FFT images (Fig. 5). The spacing of the buckling pattern decreased further to 4.5 ± 0.3 μm when water treatment was used. The spacing value corresponds to an elastic modulus of 6.5 ± 2.0 GPa for the methanol-treated ultrathin silk fibroin films. This value is about three-fold higher than that for the thicker spin-cast films and close to the values usually reserved for tough polymeric materials with rigid segments in their

Table 1. Mechanical properties of silk fibroin thin films with different fabrication processes.

Films [a]	AFM thickness [nm]	Buckling wavelength [μm]	Buckling modulus [GPa]	Bulging modulus [GPa]	Bulging residual stress [MPa]
Cast film	430	21±6	2.8±0.6	[b]	NA
LbL, water treated	85	4.5±0.3	3.4±1.5	4.2±1.3	10–20
LbL, methanol treated	102	6.1±0.4	6.5±2.0	8.6±2.1	20–30

[a] All films have been dried under identical conditions after treatments. [b] Films cannot sustain residual stresses after transfer to an open-hole substrate.

ADVANCED FUNCTIONAL MATERIALS

backbones (Table 2) [19,21,42–45]. In the case where water treatment was used, the elastic modulus decreased twofold to 3.4±1.5 GPa, which is closer to more common value for macromolecular materials and indicates reduced strength because of a lower degree of crystallinity.

Table 2. Comparison of mechanical properties of *B. mori* silk LbL nanoscale thin film to several types of materials from the literature [19,21,42–45].

Material	Form	Elastic modulus [GPa]	Ultimate stress [MPa]	Ultimate strain [%]	References
B. mori silk fibroin	Ultrathin films	6–8	100	0.5-3.0	This work
B. mori silk fibroin	fiber mats	1.6	510–650	~32	43,44
Spider silk (dragline)	fiber	4	–	35	5
Collagen	film	0.002–0.046	0.9–7.4	24–68	63
Collagen X-linked	film	0.4–0.8	47–72	12–16	63
Polylactic acid (PLA)	sheet	1.2–4.0	28–50	2–6	42,45
ABS	plate	2.1	40	25	42
PMMA	plate	2.4–3.1	55–76	2–5	42

2.4. Mechanical Properties of Silk Fibroin Films under Tensile Stress

Alternative testing of mechanical properties in tensile strain mode was tried on silk fibroin films. The pressure applied to one side of the film causes deflection, which is monitored by interferometry.[33] The bulging tests have been widely used for measuring the mechanical properties of freely suspended ultrathin films of different type with detailed description of this test given in a number of papers.[32–34,39] The results obtained are in a good agreement with that obtained other methods by other groups when applicable (tensile test, buckling method, and AFM nanomechanical probing). It is widely accepted that the bulging test is a robust and consistent method for studying mechanical properties of ultrathin films when it can be applied.[46]

It should be noted that such bulging tests of spin-cast silk fibroin films are technically challenging because of the film preparation and assembly. We observed a very poor adhesion between the silk film and the copper substrate, which prevents completion of such experiments. This problem can be caused by the rough surface of the cast film. On the other hand, the mechanical properties of ultrathin LbL silk films could be obtained by bulging the ultrathin films that were freely suspended over the 150 μm opening (Fig. 6). Figure 6 shows optical interference images of deflected silk films at different pressures. The overall pressure-deflection curve (see Fig. 7a) can be utilized to derive the micromechanical properties of the silk fibroin LbL films, such as elastic modulus, residual stress, and toughness by using the theory of the elastic deformation of freely suspended plates.[47] The elastic modulus determined from this plot was 6.5±2.0 GPa for the methanol-treated silk films. Therefore, the comparison indicated similar mechanical behavior of silk films under compressive and tensile stresses. By converting initial data to stress–strain plots according to elastic deformation theory, the ultimate strength, ultimate strain, and the toughness of the films deformed to the limits of rupture can also be determined (Fig. 7b). Overall, we obtained an elastic modulus of 8.6±2.1 GPa for the methanol-treated silk LbL films, which is close to, though a little larger than, that from the buckling tests. The systematically larger value in the bulging test could be due to the rather simple model that we applied in the analysis of the buckling patterns. However, it may also serve as an indication of the difference in tensile and compressive behavior of confined silk materials. The difference in the state of the films can also affect the results: the air–film–air confinement for the bulging test (two free surfaces) is replaced with an air–film–substrate arrangement for the buckling test. Finally, slightly different drying conditions for the freely suspended film on the copper substrate in the bulging tests and the direct contact with the hydrophobic PDMS surface in the buckling tests could cause different residual stresses. Further studies are required to clarify this discrepancy.

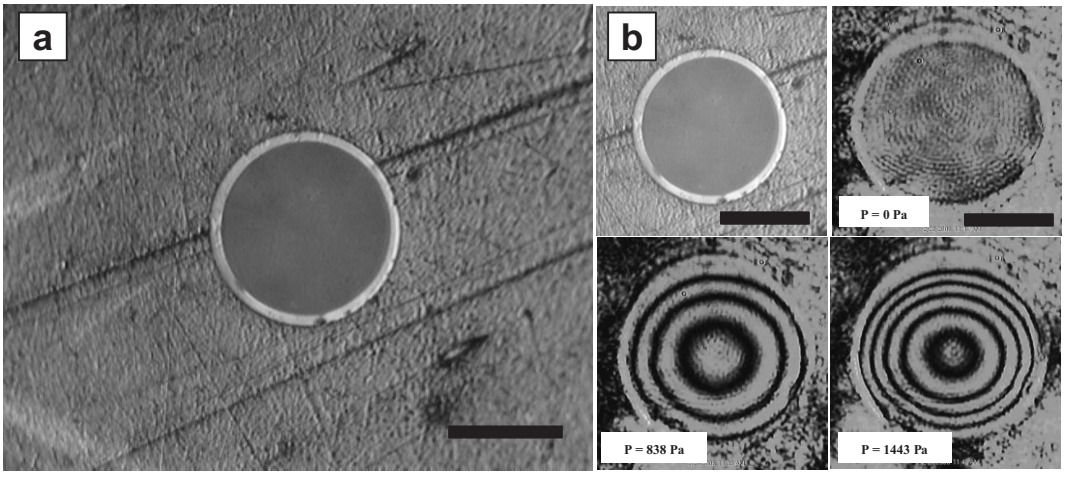

Figure 6. a) Image of a robust, uniform, and freely suspended silk fibroin LbL film over the 150 μm opening. b) Interference patterns of deformed silk films under various pressures. All scale bars are 100 μm.

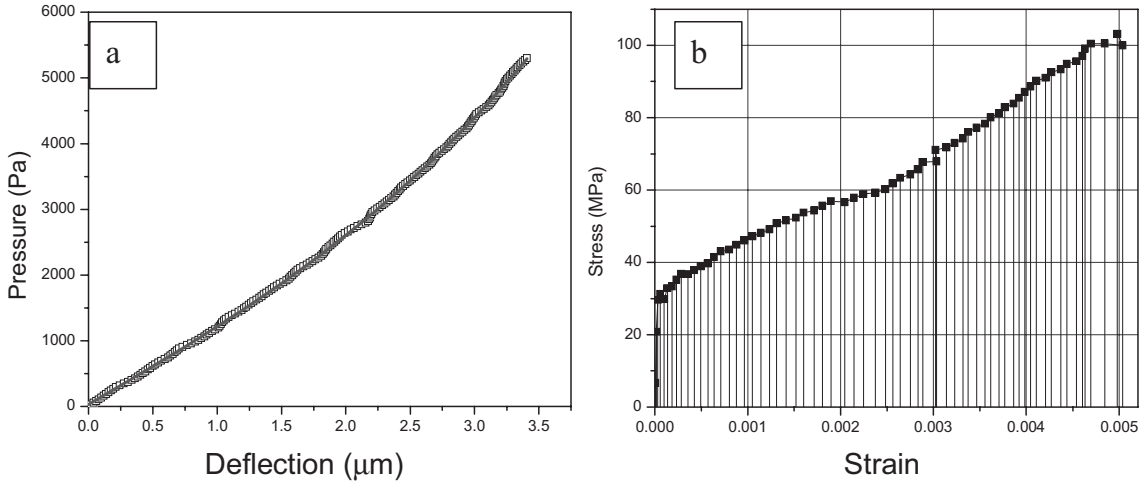

Figure 7. a) Pressure-deflection plot of methanol-treated silk fibroin LbL film; b) stress–strain curve of the silk film.

From this analysis the ultimate strength of the methanol-treated ultrathin silk films was estimated at about 100 MPa, with an ultimate strain around 0.5 % (Fig. 7b). Both values are outstanding for such ultrathin films and demonstrate excellent mechanical properties for the multilayered silk films. It is worth noting that water treatment resulted in more elastic behavior with an ultimate strain exceeding 3 % and ultimate strength exceeding 100 MPa, both parameters exceeding the measuring limits of our instrumentation (Table 1).

2.5. Molecular Structure Analysis

Attenuated total reflection-Fourier transform infrared spectroscopy (ATR-FTIR) and X-ray diffraction measurements were conducted on the multilayered films with the different processing treatments to elucidate which microstructural changes might be responsible for the difference in the mechanical properties observed above. Additional microstructural characterization techniques, such as Raman spectroscopy, can not be exploited here since the overall thickness of the ultrathin silk films is well below 100 nm, which prevents any meaningful Raman measurements.

The FTIR-ATR spectra of a spin-cast film, SA-LbL film (water treated), and SA-LbL film (methanol treated) provide very reasonable information and are shown in Figure 8. All these spectra possess a peak around 1538 cm^{-1}, which is assigned to the amorphous structure. However, FTIR spectra of the LbL films show an amide I band with a strong peak centered at 1629 cm^{-1}. Such a peak can not be observed in the spectrum of the spin-cast film. As we know, this peak is characteristic of antiparallel β-structure frequencies.[48–50] Therefore, we believe that the β-sheet structure typical for silk II can be formed in both the thin and ultrathin silk films in the process of the fabrication (although with small domain sizes) even without additional methanol treatment.

The presence of the β-sheets in the films was additionally confirmed by wide-angle X-ray diffraction (Fig. 9). Although

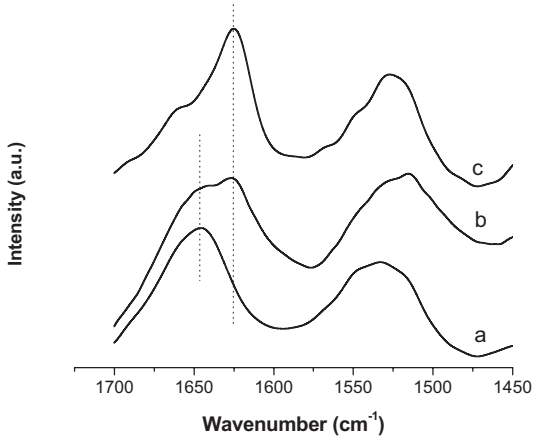

Figure 8. ATR-FTIR spectra of silk films fabricated by different processing methods: a) cast silk film, b) water-treated LbL film, c) methanol-treated LbL film.

broad maxima are observed for the spin-cast films that are indicative of a disordered structure, there is a main peak at about 21° and a shoulder at about 24°, which is a clear indication of the presence of two preferential intermolecular interactions in the lateral packing of the backbones with crystalline spacings of 0.435 and 0.37 nm, respectively. This type of shape represents the coexistence of an amorphous matrix and poorly ordered domains with crystalline structure formed by β-sheets (silk II form).[51,52] Silk II is an antiparallel β-sheet in which the polypeptide chains are aligned and adjacent chains are connected by hydrogen bonds between carbonyl and amine groups. The amino acid repeat unit in *B. mori* silkworm cocoon silk fibroin is responsible for the formation of β-sheets and consists of the sequence $GAGAGSGAAG[SGAGAG]_8Y$ (where G = glycine, A = alanine, S = serine, Y = tyrosine) with variations within subdomains of this sequence separated by less regular domains with a coiled conformation forming a less crystalline phase.[53,54] The β-sheet structure was more pronounced in

ADVANCED FUNCTIONAL MATERIALS

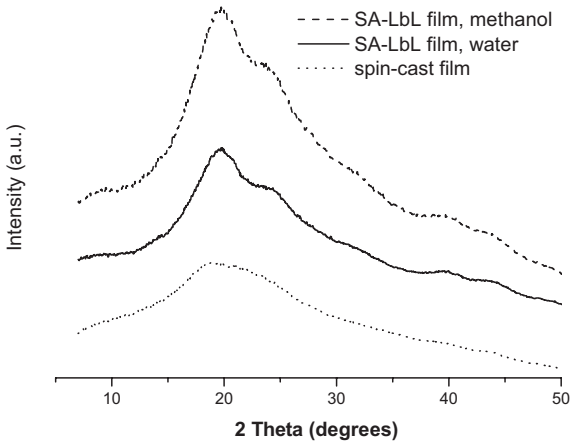

Figure 9. XRD patterns of silk films fabricated by different processing methods. Cast silk film, water-treated LbL film, and methanol-treated LbL film.

the ultrathin LbL films based on the sharper maxima and their higher intensities (Fig. 9). The formation of weakly crystalline silk II during fabrication of thin, spin-cast films could be induced during the drying process due to dehydration effects as discussed for bulk silk films.[2,55–57] Methanol treatment of the ultrathin LbL films resulted in increased β-sheet content as evident from sharper and more intense peaks by FTIR and X-ray diffraction (Figs. 8,9). The formation of these crystalline domains results in reinforcement of the materials by a network of physical crosslinks, increasing elastic modulus, ultimate strength, and film toughness (Fig. 1, Table 1).

The high values of the elastic modulus (3–4 GPa for untreated, as-prepared silk films and 6–9 GPa for methanol-treated silk films) and the ultimate strength obtained here are consistent with those obtained from independent measurements with a nano-indentation technique for identical silk fibroin as well as for other silk materials.[58,59] Indeed, for dragline silk fibroin the reported elastic moduli range from 6–8 GPa to 8–10 GPa across and along fibrils. For silk fibroin from *B. mori*, the indentation experiment revealed elastic moduli ranging from 6 to 10 GPa depending upon treatment conditions with variations caused by the partial/full transformation from silk I to silk II structures. On the other hand, the analysis of the stress–strain curve gave a toughness value for the 6-layers silk fibroin film studied here of 324 kJ m^{-3}, which is close to that reported for dragline silk fibroin (ca. 300 kJ m^{-3}).[60] Thus, we can conclude that the mechanical strength of the ultrathin silk film is not compromised by the confined state of the silk backbone and limited dimensions of the hard domains formed by the β-sheets.

However, the analysis of the ultimate elasticity (the elongation to break) shows that, unlike thick films and fibrillar materials, the ultrathin silk films studied here show much lower ultimate stretching. In fact, the range of ultimate elongation achieved for these films is within 0.5–3 % which is significantly lower than the elongation of 20–30 % routinely achieved for bulk silk materials and oriented fibrils.[60] This significant (10-fold) reduction of the ultimate elasticity indicates the inability of the silk backbones to reorient themselves via a slipping motion and, ultimately, to undergo a full-scale unfolding transformation with a step-by-step stretching of the soft and hard domains with stretching of the backbones as a result, as was discussed earlier.[61] Apparently, the confinement of multidomain backbones into ultrathin films with thicknesses comparable to the extended length of the domains (11 nm for soft domains and several hundred nanometers for hard domains[61]) imposes severe limitations on the unfolding behavior and hinders the dynamics of the chain unfolding and domain reorganization for large deformations. We suggest that such spatial constraints are instrumental in modifying the mechanical behavior of silk materials in the form of ultrathin films. In this state, silk chains become less elastic but preserve their outstanding mechanical strength.

The tensile stress, ultimate strain, and toughness of the ultrathin LbL silk films are outstanding when compared to other biomaterials and synthetic polymers. For example, polyaminosaccharides, which are widely used as a biocompatible, biodegradable, and renewable materials do not display such spectacular mechanical properties at all (Table 2).[62] As seen in Table 2, collagen possesses a very low tensile strength not exceeding 50 MPa combined with a very low elastic modulus. Even crosslinked collagen films show an elastic modulus that is still an order of magnitude lower and an ultimate strength that is twice as low as those for the silk films studied here.[63] Another popular biocompatible polymer, polylactic acid (PLA), also shows mechanical properties that are several times lower than those reported here (Table 2). Finally, the ultrathin LbL films studied here demonstrate tensile strengths and elastic moduli comparable or higher to those of high-performance composite materials and glassy polymers such as acrylonitrile butadiene styrene (ABS) plastics and poly(methyl methacrylate) (PMMA).[42] This better performance is also accompanied by an outstanding toughness that is manifold higher than that usually observed for conventional polymer composites (328 kJ m^{-3} for the silk material studied here versus typical values below 100 kJ m^{-3}).

3. Conclusions

The mechanical properties of thin silk films fabricated with traditional spin casting and ultrathin films fabricated with spin-assisted LbL deposition were assessed after a variety of different post-processing treatments. Outstanding mechanical properties were observed for ultrathin silk films with thicknesses below 100 nm, both in compressive and tensile modes. These films were characterized by a high elastic modulus of 6.5 GPa and ultimate strength reaching 100 MPa after methanol treatment, because of the formation of a reinforced microstructure with crystalline β-sheets serving as the reinforcing fillers and physical crosslink sites similar to bulk silk materials. However, the confined state of the silk backbones within films thinner than the lengths of the extended domains causes a reduced elasticity of the film albeit without compromising their me-

chanical strength, which should be considered in the design of nanoscale films from silk materials. These regenerated silk fibroin LbL films with outstanding mechanical properties and potential biocompatibility should provide value to a number of bio-related devices in the future.

4. Experimental

Silkworm cocoon silk fibroin from *B. mori* contains two structural proteins, namely a fibroin "heavy" chain with a molecular weight of about 390 000 Da and a fibroin "light" chain with a molecular weight of about 25 000 Da [53]. These two proteins are linked by a single disulfide bond to form a large protein chain that remains linked during protein processing into fibers by the silkworm and may play a role in the regulation of chain folding and fiber formation.

For the first solution, the silk was obtained from *B. mori* silkworms raised on a diet of Silkworm Chow (Mullberry Farms, Fallbrook, CA). Live pupae were extracted from the cocoons prior to sericin removal in order to avoid contamination of the fibroin protein. Silk fibers were prepared as previously described [64,65]. Briefly, silkworm cocoons were soaked at 3.3 % (w/v) in a solution of 8 M urea, 40 mM Tris-SO_4, and 0.5 M β-mercaptoethanol, and were heated to 90 °C for 1 hr. The silk fiber was then extensively washed with ultrapure distilled water (18 MΩ cm) and dried overnight under vacuum. Extracted silk fibroin fibers were dissolved in 1-butyl-3-methylimidazolium chloride (BMIC) ionic liquid (io-li-tec GmbH and Co, Denzlingen, Germany) to form a 10 % (w/w) solution. Dissolution was carried out by heating a mixture of the silk fiber and BMIC powder to 90 °C for 1 hr. The fiber and ionic liquid were then mixed for 30 s in a speed mixer (FlackTek Inc., Landrum, SC) and returned to heating at 90 °C for 1 hr. The mixing and heating steps were repeated four times. Water, 25 % (w/w), was added to the heated solution in order to lower the viscosity and melting point. The final composition of the solution was 7.5 % (w/w) silk fibroin, 25 % (w/w) water, and 67.5 % (w/w) BMIC.

For the second silk fibroin solution (aqueous solution, 8 % w/v), the samples were prepared following our previously published methods [66] and kept in the refrigerator before use. Cocoons of *B. mori* silkworms were kindly supplied by M. Tsukada, Institute of Sericulture (Tsukuba, Japan). The silk fibroin aqueous stock solution was prepared as previously described [67]. Briefly, cocoons were boiled for 30 min in an aqueous solution of 0.02 M Na_2CO_3 and then rinsed thoroughly with distilled water to extract the glue-like sericin proteins. The extracted silk fibroin was dissolved in 9.3 M LiBr solution at 60 °C for 4 h, yielding a 20 wt % solution. The solution was dialyzed against distilled water using Slide-a-Lyzer dialysis cassettes (MWCO 3500, Pierce) at room temperature for 3 days to remove the salt. The dialysate was centrifuged three times, each at –20 °C for 20 min, to remove impurities and aggregates that occurred during dialysis. The final concentration of the silk fibroin aqueous solution was approximately 8 wt %. The solution was diluted to the desired working solution with deionized (DI) water for thin-film fabrication and LbL assembly.

First, a series of spin-cast and SA-LbL films were prepared by spin-coating silk solutions onto a silicon wafer, which was freshly cleaned with published procedures adapted in the laboratory [68]. Second, for the fabrication of free-standing films, the viscous silk fibroin solution was deposited on top of a sacrificial cellulose acetate (CA) layer with a speed of 3000 rpm on a PM101DT-R485 spinner (Headway Research, Inc., Garland, TX). The sacrificial layer was deposited on the silicon wafer from a 2 % acetone solution. For this deposition the silk solution was diluted to 2.0 mg mL^{-1} and about 200 μL of the solution was used for each deposited layer. The silk films on the substrate were then rinsed with methanol or water and dried overnight before being released. Freely suspended silk fibroin films were obtained by dissolving the sacrificial layers in acetone as described elsewhere [69]. To increase the β-sheet crystal formation in the films, in most cases methanol was used to rinse the films before final drying. The fabrication processes were conducted in a class 100 clean room and ultrapure water with a resistivity of 18 MΩ cm was used in all experiments.

The morphology and surface roughness of the silk fibroin LbL films were investigated with a Dimension 3000 atomic force microscope (AFM) (Digital Instruments) in the tapping mode according to procedures adapted in the laboratory [68]. AFM images of the silk film edge were collected and analyzed with both bearing and step analysis to obtain film thickness. The thickness of the silk film was also obtained with a COMPEL automatic ellipsometer (InOmTech, Inc.) at an incident angle of 70°. The refractive index of silk fibroin was 1.5 by comparing AFM and ellipsometry measurements. The refractive index of the silk films was also measured by prism-coupled laser light onto films of uniform thicknesses using three different laser wavelengths of 632 nm, 1152 nm, and 1523 nm and was calculated to be ca. 1.54, which is similar to the values given in the literature (1.56) [70,71].

The mechanical properties of the silk films were measured with both buckling and bulging tests. It should be noted that despite the fact that the release procedure during the fabrication of the free-standing silk films might affect the mechanical properties of the silk films we did not observe any noticeable deterioration of the microstructure and properties. The mechanical properties obtained here are for silk films after the dissolving of the sacrificial layer with acetone solvent. The effect of the chemical treatment on the silk films is an interesting subject and will be studied and reported elsewhere. A home-made bulging setup with an interference optical system was used to conduct bulging tests as described previously [69]. The pressure differential applied to the freely suspended silk fibroin films was monitored with a digital pressure modulus (DPM-0.1, SI Pressure Instruments Ltd, Birmingham, UK) with an accuracy of 2 Pa. The mechanical deflections in the out-of-plane direction were monitored and the interference pattern was recorded by a CCD camera. The elastic modulus, residual stress, and toughness of the silk fibroin films were achieved by analysis of the pressure-deflection curves using the model of elastic deformation of a circular plate clamped to a stiff edge, as being detailed in the literature [47]. For buckling tests, the freely suspended silk fibroin LbL films fabricated on a sacrificial layer were transferred onto an elastic PMDS substrate, which was then compressed to induce the buckling instability patterns. The elastic moduli of the PDMS substrates were measured with conventional tensile tests. The bucking patterns were observed with a Leica DM 4000 microscope in reflection mode with a 50× objective and recorded with a high-resolution camera. The periodicity of the buckling patterns was obtained by fast Fourier transform using Image-J software.

The silk fibroin conformation in the LbL films was studied by ATR-FTIR (Equinox 55; Bruker, Billerica, MA). The structure of the films was analyzed with a Bruker D8 Discover X-ray diffractometer with a general area diffraction detection system (GADDS) multiwire area detector. Wide-angle X-ray diffraction (WAXD) experiments were performed employing Cu Kα radiation (40 kV and 20 mA).

Received: November 25, 2006
Revised: May 24, 2007
Published online: August 2, 2007

[1] Z. Shao, F. Vollrath, *Nature* **2002**, *418*, 741.
[2] H.-J. Jin, D. L. Kaplan, *Nature* **2003**, *424*, 1057.
[3] F. Vollrath, B. Madsen, Z. Shao, *Proc. R. Soc. Lond. B* **2001**, *268*, 2339.
[4] X. Chen, Z. Shao, F. Vollrath, *Soft Matter* **2006**, *2*, 448.
[5] R. V. Lewis, *Chem. Rev.* **2006**, *106*, 3762.
[6] D. L. Kaplan, S. J. Lombardi, S. A. Fossey, in *Biomaterials: Novel Materials from Biological Sources* (Ed: D. Byrom), Stockton Press, New York, NJ **1991**, Ch. 1.
[7] K. Ohgo, C. Zhao, M. Kobayashi, T. Asakura, *Polymer* **2003**, *44*, 841.
[8] D. L. Kaplan, W. W. Adams, B. Farmer, C. Viney, *Silk Polymers: Material Science and Biotechnology*, *ACS Symp. Ser. 544*, American Chemical Society, Washington, DC **2001**, Ch. 29.
[9] Y. Iridag, M. Kazanci, *J. Appl. Polym. Sci.* **2006**, *100*, 4260.
[10] L. Zhou, X. Chen, W. Dai, Z. Shao, *Biopolymers* **2006**, *82*, 144.
[11] G. H. Altman, F. Diaz, C. Jakuba, T. Calabro, R. L. Horan, J. Chen, H. Lu, J. Richmond, D. L. Kaplan, *Biomaterials* **2003**, *24*, 401.

[12] W. H. Park, W. S. Ha, H. Ito, T. Inagaki, Y. Noishiki, *Fibers Polym.* **2001**, *2*, 58.
[13] M. Li, W. Tao, S. Lu, S. Kuga, *Int. J. Biol. Macromolecules* **2003**, *23*, 159.
[14] K.-H. Kim, L. Jeong, H.-N. Park, S.-Y. Shin, W.-H. Park, S.-C. Lee, T.-I. Kim, Y.-J. Park, Y.-J. Seol, Y.-M. Lee, Y. Ku, I.-C. Rhyu, S.-B. Han, C.-P. Chung, *J. Biotechnol.* **2005**, *120*, 327.
[15] H.-J. Jin, J. Park, V. Karageorgiou, U.-J. Kim, R. Valluzzi, P. Cebe, D. L. Kaplan, *Adv. Funct. Mater.* **2005**, *15*, 1241.
[16] X. Wang, H. J. Kim, P. Xu, A. Matsumoto, D. L. Kaplan, *Langmuir* **2005**, *21*, 11 335.
[17] T. Arai, G. Freddi, R. Innocenti, M. Tsukada, *J. Appl. Polym. Sci.* **2004**, *91*, 2383.
[18] M. K. Gupta, S. K. Khokhar, D. M. Phillips, L. A. Sowards, L. F. Drummy, M. P. Kadakia, R. R. Naik, *Langmuir* **2007**, *23*, 1315.
[19] J. M. Gosline, M. E. DeMont, M. W. Denny, *Endeavour* **1986**, *10*, 37.
[20] J. M. Gosline, M. W. Denny, M. E. DeMont, *Nature* **1984**, *309*, 551.
[21] P. M. Cunniff, S. A. Fossey, M. A. Auerbach, J. W. Song, D. L. Kaplan, W. W. Adams, R. K. Eby, D. Mahoney, D. L. Vezie, *Polym. Adv. Technol.* **1994**, *5*, 401.
[22] J. Pérez-Rigueiro, C. Viney, J. Llorca, M. Elices, *J. Appl. Polym. Sci.* **2000**, *75*, 1270.
[23] J. Pérez-Rigueiro, C. Viney, J. Llorca, M. Elices, *J. Appl. Polym. Sci.* **1998**, *70,* 2439.
[24] S. Das, A. Ghosh, *J. Appl. Polym. Sci.* **2006**, *99*, 3077.
[25] N. Agarwal, D. A. Hoagland, R. J. Farris, *J. Appl. Polym. Sci.* **1997**, *63*, 401.
[26] X. Wang, Y.-G. Kim, C. Drew, B.-C. Ku, J. Kumar, L. A. Samuelson, *Nano Lett.* **2004**, *4*, 331.
[27] D. M. Lynn, *Soft Matter* **2006**, *2*, 269.
[28] A. A. Antipov, G. B. Sukhorukov, *Adv. Colloid Interf. Sci.* **2004**, *111*, 49.
[29] L. Zhai, M. C. Berg, F. C. Cebeci, Y. Kim, J. M. Milwid, M. F. Rubner, R. E. Cohen, *Nano Lett.* **2006**, *6*, 1213.
[30] T. R. Farhat, P. T. Hammond, *Adv. Funct. Mater.* **2005**, *15*, 945.
[31] a) J. Cho, K. Char, J.-D. Hong, K.-B. Lee, *Adv. Mater.* **2001**, *13*, 1076. b) P. A. Chiarelli, M. S. Johal, J. L. Carron, J. B. Roberts, J. M. Robinson, H.-L. Wang, *Adv. Mater.* **2001**, *13*, 1167.
[32] a) C. Jiang, S. Markutsya, V. V. Tsukruk, *Adv. Mater.* **2004**, *16*, 157. b) C. Jiang, S. Markutsya, V. V. Tsukruk, *Langmuir* **2004**, *20*, 882. c) C. Jiang, S. Markutsya, Y. Pikus, V. V. Tsukruk, *Nature Mater.* **2004**, *3*, 721.
[33] a) C. Jiang, S. Markutsya, H. Shulha, V. V. Tsukruk, *Adv. Mater.* **2005**, *17*, 1669. b) H. Ko, C. Jiang, V. V. Tsukruk, *Chem. Mater.* **2005**, *17*, 2490. c) R. Gunawidjaja, C. Jiang, S. Seleshanko, M. Ornatska, S. Singamaneni, V. V. Tsukruk, *Adv. Funct. Mater.* **2006**, *16*, 2024.
[34] a) C. Jiang, W. Y. Lio, V. V. Tsukruk, *Phys. Rev. Lett.* **2005**, *95*, 115 503. b) C. Jiang, D. S. Kommireddy, V. V. Tsukruk, *Adv. Funct. Mater.* **2006**, *16*, 27.
[35] a) C. Jiang, V. V. Tsukruk, *Adv. Mater.* **2006**, *18*, 829. b) C.Jiang, V. V. Tsukruk, *Soft Matter* **2005**, *1*, 334.
[36] C. M. Stafford, C. Harrison, K. L. Beers, A. Karim, E. J. Amis, M. R. VanLandingham, H. Kim, W. Volksen, R. D. Miller, E. E. Simonyi, *Nature Mater.* **2004**, *3*, 545.
[37] J. Genzer, J. Groenewold, *Soft Matter* **2006**, *2*, 310.
[38] M. W. Moon, K. R. Lee, K. H. Oh, J. W. Hutchinson, *Acta Mater.* **2004**, *52*, 3151.
[39] A. J. Nolte, M. F. Rubner, R. E. Cohen, *Macromolecules* **2005**, *38*, 5367.
[40] C. Jiang, S. Singamaneni, E. Merrick, V. V. Tsukruk, *Nano Lett.* **2006**, *6*, 2254.
[41] *Polymeric Multicomponent Materials: An Introduction*, 2nd ed. (Ed: L. H. Sperling), Wiley-VCH, Weinheim, Germany **1997**.
[42] *Polymer Handbook*, 4th ed. (Eds: J. Brandrup, E. H. Immergut, E. A. Grulke), John Wiley & Sons, Inc., New York, NJ **1999**.
[43] G. D. Pins, D. L. Christiansen, R. Patel, F. H. Silver, *Biophys. J.* **1997**, *73*, 2164.
[44] J. Ayutsedea, M. Gandhib, S. Sukigarac, M. Micklusa, H.-E. Chen, F. Ko, *Polymer* **2005**, *46*, 1625.
[45] B. Gupta, N. Revagade, N. Anjum, B. Atthoff, J. Hilborn, *J. Appl. Polym. Sci.* **2006**, *101*, 3774.
[46] Y. Xiang, X. Chen, T. Y. Tsui, J.-I. Jang, J. J. Vlassak, *J. Mater. Res.* **2006**, *21*, 386.
[47] R. Gunawidjaja, C. Jiang, H. Ko, V. V. Tsukruk, *Adv. Mater.* **2006**, *18*, 1895.
[48] O. N. Tretinnikov, O. Y. Tamada, *Langmuir* **2001**, *17*, 7406.
[49] C. Mouro, C. Jung, A. Bondon, G. Simonneaux, *Biochemistry* **1997**, *36*, 8125.
[50] A. Matsumoto, H. J. Kim, I. Tsai, X. Wang, P. Cebe, D. L. Kaplan, *Polym. Rev.* **2007**, *1*, 29.
[51] R. Valluzzi, H. J. Jin, *Biomacromolecules* **2004**, *5*, 696.
[52] I. C. Um, C. S. Ki, H. Y. Kweon, K. G. Lee, D. W. Ihm, Y. H. Park, *Int. J. Biol. Macromol.* **2004**, *34*, 107.
[53] C. Z. Zhou, F. Confalonieri, N. Medina, Y. Zivanovic, C. Esnault, T. Yang, M. Jacquet, J. Janin, M. Duguet, R. Perasso, Z. G. Li, *Nucleic Acids Res.* **2000**, *28*, 2413.
[54] K. Mita, S. Ichimura, T. C. James, *J. Mol. Evol.* **1994**, *38*, 583.
[55] R. Valluzzi, S. P. Gido, W. P. Zhang, W. S. Muller, D. L. Kaplan, *Macromolecules* **1996**, *29*, 8606.
[56] J. Magoshi, Y. Magoshi, M. A. Becker, S. Nakamura, in *Materials Encyclopedia* (Ed: J. C. Salamone), CRC Press, New York, NJ **1996**, p. 667.
[57] J. Nam, Y. H. Park, *J. Appl. Polym. Sci.* **2001**, *81*, 3008.
[58] D. M. Ebenstein, K. J. Wahl, *J. Mater. Res.* **2006**, *21*, 2035.
[59] D. M. Ebenstein, J. Park, D. L. Kaplan, K. J. Wahl, *MRS Symp. Ser.* **2005**, *841*, 57.
[60] R. V. Lewis, *Chem. Rev.* **2006**, *106*, 3762.
[61] H. Shulha, C. Wong, D. L. Kaplan, V. V. Tsukruk, *Polymer* **2006**, *47*, 5821.
[62] J. K. Suh, H. W. T. Matthew, *Biomaterials* **2000**, *21*, 2589.
[63] P. Mallika, A. Himabindu, D. Shailaja, *J. Appl. Polym. Sci.* **2006**, *101*, 63.
[64] D. M. Phillips, L. F. Drummy, D. G. Conrady, D. M. Fox, R. R. Naik, M. O. Stone, P. C. Trulove, H. C. De Long, R. A. Mantz, *J. Am. Chem. Soc.* **2004**, *126*, 14 350.
[65] D. M. Phillips, L. F. Drummy, R. R. Naik, H. C. De Long, D. M. Fox, P. C. Trulove, R. A. Mantz, *J. Mater. Chem.* **2005**, *15*, 4206.
[66] U.-J. Kim, J. H. Park, H. J. Kim, M. Wada, D. L. Kaplan, *Biomaterials* **2005**, *26*, 2775.
[67] S. Sofia, M. B. McCarthy, G. Gronowicz, D. L. Kaplan, *J. Biomed. Mater. Res.* **2001**, *54*, 139.
[68] V. V. Tsukruk, V. N. Bliznyuk, *Langmuir* **1998**, *14*, 446.
[69] S. Markutsya, C. Jiang, Y. Pikus, V. V. Tsukruk, *Adv. Funct. Mater.* **2005**, *15*, 771.
[70] M. Tsukada, K. Hirabayashi, *J. Polym. Sci.: Polym. Lett. Ed.* **1980**, *18*, 507.
[71] A. A. Hamza, I. M. Fouda, T. Z. Sokkar, M. A. El-Bakary, *Egypt. J. Appl. Polym. Sci.* **1996**, *60*, 1289.